Research Article
NAFLD and Alcohol-Related Liver Diseases

JOURNAL
OF HEPATOLOGY

Macrophage scavenger receptor 1 mediates lipid-induced inflammation in non-alcoholic fatty liver disease

Graphical abstract

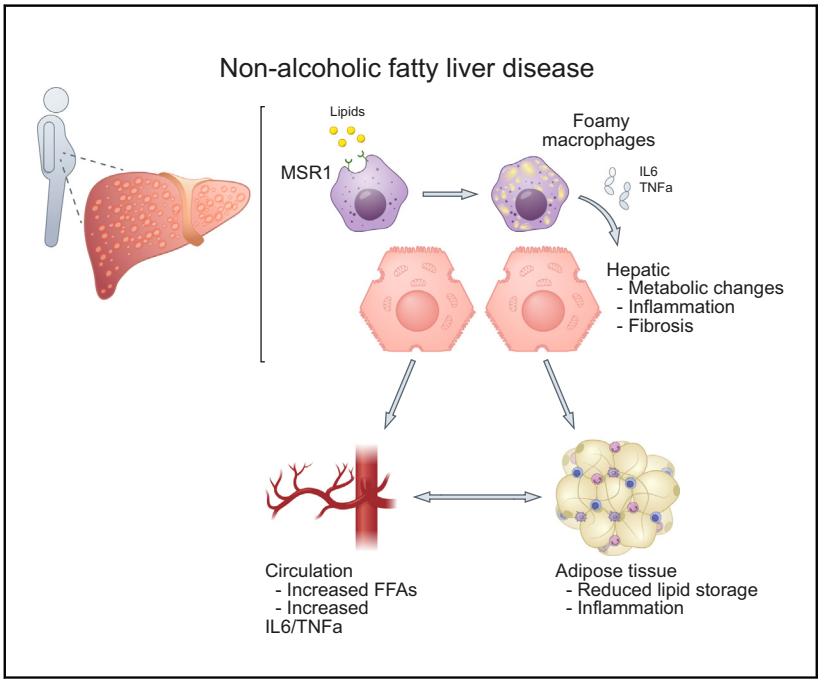

Highlights

- In human NAFLD, MSR1 is expressed in mature Kupffer cells and foamy macrophages.
- *MSR1* transcript levels are associated with disease activity in patients with NAFLD.
- Mice lacking Msr1 are protected from diet-induced metabolic disorder.
- Uptake of saturated fatty acids via MSR1 results in a pro-inflammatory response.
- The SNP rs41505344 upstream of MSR1 is associated with altered serum triglycerides.

Authors

Olivier Govaere, Sine Kragh Petersen, Nuria Martinez-Lopez, …, Quentin M. Anstee, Matthias Trost, Anetta Härtlova

Correspondence

olivier.govaere@newcastle.ac.uk (O. Govaere), quentin.anstee@newcastle.ac.uk (Q.M. Anstee), matthias.trost@newcastle.ac.uk (M. Trost), anetta.hartlova@gu.se (A. Härtlova).

Lay summary

Non-alcoholic fatty liver disease (NAFLD) is a chronic disease primarily caused by excessive consumption of fat and sugar combined with a lack of exercise or a sedentary lifestyle. Herein, we show that the macrophage scavenger receptor MSR1, an innate immune receptor, mediates lipid uptake and accumulation in Kupffer cells, resulting in liver inflammation and thereby promoting the progression of NAFLD in humans and mice.

https://doi.org/10.1016/j.jhep.2021.12.012
 J. Hepatol. 2022, 76, 1001–1012

Research Article
NAFLD and Alcohol-Related Liver Diseases

JOURNAL OF HEPATOLOGY

Macrophage scavenger receptor 1 mediates lipid-induced inflammation in non-alcoholic fatty liver disease

Olivier Govaere[1,*,†], Sine Kragh Petersen[2,‡], Nuria Martinez-Lopez[3,4,‡], Jasper Wouters[5,6], Matthias Van Haele[7], Rosellina M. Mancina[8], Oveis Jamialahmadi[8], Orsolya Bilkei-Gorzo[2], Pierre Bel Lassen[9], Rebecca Darlay[10], Julien Peltier[11], Jeremy M. Palmer[1], Ramy Younes[1,12], Dina Tiniakos[1,13], Guruprasad P. Aithal[14], Michael Allison[15], Michele Vacca[16], Melker Göransson[17], Rolando Berlinguer-Palmini[18], James E. Clark[1], Michael J. Drinnan[1], Hannele Yki-Järvinen[19], Jean-Francois Dufour[20,21], Mattias Ekstedt[22], Sven Francque[23], Salvatore Petta[24], Elisabetta Bugianesi[12], Jörn M. Schattenberg[25], Christopher P. Day[1], Heather J. Cordell[10], Baki Topal[26], Karine Clément[9], Stefano Romeo[8], Vlad Ratziu[27], Tania Roskams[7], Ann K. Daly[1], Quentin M. Anstee[1,28,*,†], Matthias Trost[11,*,†], Anetta Härtlova[2,11,*,†]

[1]Translational and Clinical Research Institute, Faculty of Medical Sciences, Newcastle University, Newcastle upon Tyne, United Kingdom; [2]Wallenberg Centre for Molecular and Translational Medicine, Department of Microbiology and Immunology at Institute of Biomedicine, University of Gothenburg, Gothenburg, Sweden; [3]Department of Medicine, Albert Einstein College of Medicine, Bronx, NY 10461, USA; [4]Department of Radiation Oncology, Albert Einstein College of Medicine, Bronx, NY 10461, USA; [5]Center for Brain & Disease Research, VIB-KU Leuven, Leuven, Belgium; [6]Department of Human Genetics, KU Leuven, Leuven, Belgium; [7]Department of Imaging and Pathology, Translational Cell and Tissue Research, KU Leuven and University Hospitals Leuven, Leuven, Belgium; [8]The Wallenberg Laboratory for Cardiovascular and Metabolic Research, Department of Molecular and Clinical Medicine, University of Gothenburg, Gothenburg, Sweden; [9]Nutrition and obesity: systemic approaches, Inserm, Sorbonne University, Paris, France; [10]Population Health Sciences Institute, Faculty of Medical Sciences, Newcastle University, Newcastle upon Tyne, United Kingdom; [11]Biosciences Institute, Faculty of Medical Sciences, Newcastle University, Newcastle upon Tyne, United Kingdom; [12]Department of Medical Sciences, Division of Gastro-Hepatology, A.O. Città della Salute e della Scienza di Torino, University of Turin, Turin, Italy; [13]Department of Pathology, Aretaieio Hospital, National & Kapodistrian University of Athens, Athens, Greece; [14]NIHR Nottingham Biomedical Research Centre, Nottingham University Hospitals NHS Trust and University of Nottingham, Nottingham, United Kingdom; [15]Liver Unit, Department of Medicine, Cambridge NIHR Biomedical Research Centre, Cambridge University NHS Foundation Trust, United Kingdom; [16]University of Cambridge Metabolic Research Laboratories, Wellcome-MRC Institute of Metabolic Science, Addenbrooke's Hospital, Cambridge, United Kingdom; [17]Bioscience COPD/IPF, Research and Early Development, Respiratory and Immunology (R&I), BioPharmaceuticals R&D, AstraZeneca, Gothenburg, Sweden; [18]Bioimaging Unit, Faculty of Medical Sciences, Newcastle University, Newcastle upon Tyne, United Kingdom; [19]Minerva Foundation Institute for Medical Research and Department of Medicine, University of Helsinki, Helsinki, Finland; [20]University Clinic for Visceral Surgery and Medicine, University of Bern, Bern, Switzerland; [21]Hepatology, Department of Biomedical Research, University of Bern, Bern, Switzerland; [22]Division of Gastroenterology and Hepatology, Department of Medicine and Health Sciences, Linköping University, Linköping, Sweden; [23]Department of Gastroenterology and Hepatology, Antwerp University Hospital & University of Antwerp, Antwerp, Belgium; [24]Sezione di Gastroenterologia, Dipartimento Biomedico di Medicina Interna e Specialistica, Università di Palermo, Palermo, Italy; [25]I. Department of Medicine, University Hospital Mainz, Mainz, Germany; [26]Department of Abdominal Surgery, KU Leuven and University Hospitals Leuven, Leuven, Belgium; [27]Assistance Publique-Hôpitaux de Paris, hôpital Beaujon, University Paris-Diderot, Paris, France; [28]Newcastle NIHR Biomedical Research Centre, Newcastle upon Tyne Hospitals NHS Trust, Newcastle upon Tyne, United Kingdom

Background & Aims: Obesity-associated inflammation is a key player in the pathogenesis of non-alcoholic fatty liver disease (NAFLD). However, the role of macrophage scavenger receptor 1 (MSR1, CD204) remains incompletely understood.

Methods: A total of 170 NAFLD liver biopsies were processed for transcriptomic analysis and correlated with clinicopathological features. *Msr1*$^{-/-}$ and wild-type mice were subjected to a 16-week high-fat and high-cholesterol diet. Mice and *ex vivo* human liver slices were treated with a monoclonal antibody against MSR1. Genetic susceptibility was assessed using genome-wide association study data from 1,483 patients with NAFLD and 430,101 participants of the UK Biobank.

Results: MSR1 expression was associated with the occurrence of hepatic lipid-laden foamy macrophages and correlated with the

Keywords: macrophages; immunometabolism; NASH; inflammation.
Received 26 March 2021; received in revised form 5 December 2021; accepted 7 December 2021; available online 21 December 2021

* Corresponding authors. Addresses: Translational and Clinical Research Institute (O.G. and Q.M.A) or Biosciences Institute (M.T), The Medical School, Newcastle University, 4th Floor, William Leech Building, Framlington Place, Newcastle-upon-Tyne, NE2 4HH, United Kingdom; (O. Govaere), or (Q.M. Anstee), or (M. Trost), or Wallenberg Centre for Molecular and Translational Medicine, University of Gothenburg, Institute of Biomedicine, Department of Microbiology and Immunology Medicinaregatan 7 A, 40530 Göteborg, Sweden. (A. Härtlova).
E-mail addresses: olivier.govaere@newcastle.ac.uk (O. Govaere), quentin.anstee@newcastle.ac.uk (Q.M. Anstee), matthias.trost@newcastle.ac.uk (M. Trost), anetta.hartlova@gu.se (A. Härtlova).
† Senior authors.
‡ contributed equally.

https://doi.org/10.1016/j.jhep.2021.12.012

degree of steatosis and steatohepatitis in patients with NAFLD. Mice lacking Msr1 were protected against diet-induced metabolic disorder, showing fewer hepatic foamy macrophages, less hepatic inflammation, improved dyslipidaemia and glucose tolerance, and altered hepatic lipid metabolism. Upon induction by saturated fatty acids, MSR1 induced a pro-inflammatory response via the JNK signalling pathway. *In vitro* blockade of the receptor prevented the accumulation of lipids in primary macrophages which inhibited the switch towards a pro-inflammatory phenotype and the release of cytokines such as TNF-α. Targeting MSR1 using monoclonal antibody therapy in an obesity-associated NAFLD mouse model and human liver slices resulted in the prevention of foamy macrophage formation and inflammation. Moreover, we identified that rs41505344, a polymorphism in the upstream transcriptional region of *MSR1*, was associated with altered serum triglycerides and aspartate aminotransferase levels in a cohort of over 400,000 patients.

Conclusions: Taken together, our data suggest that MSR1 plays a critical role in lipid-induced inflammation and could thus be a potential therapeutic target for the treatment of NAFLD.

Lay summary: Non-alcoholic fatty liver disease (NAFLD) is a chronic disease primarily caused by excessive consumption of fat and sugar combined with a lack of exercise or a sedentary lifestyle. Herein, we show that the macrophage scavenger receptor MSR1, an innate immune receptor, mediates lipid uptake and accumulation in Kupffer cells, resulting in liver inflammation and thereby promoting the progression of NAFLD in humans and mice.

Introduction

With the increasing prevalence of obesity, non-alcoholic fatty liver disease (NAFLD) has become the most common chronic liver disease globally.[1] NAFLD is characterised by excessive hepatic triglyceride accumulation and represents a series of diseased states ranging from isolated steatosis (non-alcoholic fatty liver, NAFL) to non-alcoholic steatohepatitis (NASH), identified by the presence of necro-inflammation and hepatocyte ballooning, with varying degrees of fibrosis. NAFLD is strongly linked with metabolic syndrome, *i.e.* dyslipidaemia, hypertension, obesity and type 2 diabetes mellitus (T2DM), and currently affects 20% to 30% of the global population.[1] Importantly, not all patients progress from NAFL to NASH and although gene signatures of more advanced fibrosing-steatohepatitis have been identified, the exact pathogenic pathways involved in the initiating phases of the disease, especially the transition from NAFL to NASH, are not fully understood.[2]

Growing evidence supports the view that Kupffer cells, the endogenous hepatic macrophages, are initiators of inflammation and hence contribute to NAFLD development, whilst recruited monocyte-derived macrophages are often observed in advanced stages of the disease.[3] Hepatic macrophages are responsive to a variety of stimuli including bacterial endotoxins (such as lipopolysaccharide) but also free fatty acids (FFAs) or cholesterol.[4] An excess of FFAs and cholesterol can cause the formation of hepatic foamy macrophages, and lead to Kupffer cell aggregates and lipogranulomas during steatohepatitis.[5] Specifically, the intake of saturated fat has been shown to induce insulin resistance and to enhance intrahepatic triglyceride accumulation and steatohepatitis.[6]

Palmitic acid, rather than non-saturated fatty acids (non-SFAs), has been shown to be a strong inducer of inflammation in immortalised cell lines through activation of the downstream JNK signalling pathway.[7] Recent data show that pro-inflammatory activation of murine bone marrow-derived macrophages (BMDMs) by palmitic acid is independent of Toll-like receptor 4, yet the receptor that is responsible is still not known.[8] Recently, we have shown that *in vitro* activation of the phagocytic receptor, macrophage scavenger receptor 1 (MSR1, also known as SR-A or CD204), results in pro-inflammatory macrophage polarisation through JNK activation.[9] MSR1 is a key macrophage receptor for the clearance of circulating lipoproteins and has been implicated in atherogenesis.[10] In irradiated low-density lipoprotein receptor-deficient mice, transplantation of $Msr1^{-/-}/CD36^{-/-}$ monocytes reduced dietary-induced inflammation.[11] However, the molecular mechanisms underlying hepatic macrophage activation and/or the formation of foamy macrophages in NAFLD remain poorly understood. We therefore hypothesised that MSR1 might be involved in inflammatory responses in the context of lipid overload during obesity-induced NAFLD.

Materials and methods

Patient selection

Cases were derived from the European NAFLD Registry (NCT04442334), approved by the relevant Ethical Committees in the participating centres, and all patients having provided informed consent.[12] For the histopathological and nanoString® study, 194 formalin-fixed paraffin-embedded or frozen liver biopsies samples were obtained from patients diagnosed with histological proven NAFLD at the Freeman Hospital, Newcastle Hospitals NHS Foundation Trust, Newcastle-upon-Tyne, UK and at the Pitié-Salpêtrière Hospital, Paris, France (Table S1). For the genome-wide association study, 1,483 patients with histological proven NAFLD were included as previously described.[13] All liver tissue samples for the histopathological and nanoString® study were centrally scored according to the semi-quantitative NASH-CRN scoring system by an expert liver pathologist (DT).[14] Fibrosis was staged from F0 through to F4 (cirrhosis). Alternate diagnoses and aetiologies, such as excessive alcohol intake, viral hepatitis, autoimmune liver diseases and steatogenic medication use, were excluded. Viable normal human liver tissue (for the *ex vivo* slices) was obtained after resection from 2 adult patients treated at the University Hospitals Leuven, Leuven, Belgium. Samples were assessed by an expert liver pathologist (TR).

Animals

Male $Msr1^{-/-}$ or $Msr1^{+/+}$ (wild-type [WT]) C57BL/6 mice were either kindly provided by Prof. Siamon Gordon, University of Oxford or obtained from Jackson Laboratories and bred in a conventional animal facility under standard conditions. Animals received human care and experimental protocols were approved by the institutional animal ethics committees at Newcastle University (PC123A338) and University of Gothenburg (2947/20). Mice had free access to water and were fed either standard chow (n = 10, 5 WT and 5 $Msr1^{-/-}$) or 45%-high-fat and high-cholesterol diets (HFD; 820263, Special Diet Services; n = 10, 5 WT and 5 $Msr1^{-/-}$) *ad libitum*. For the therapeutic intervention, WT mice were put on a 12-week HFD and intravenously injected with

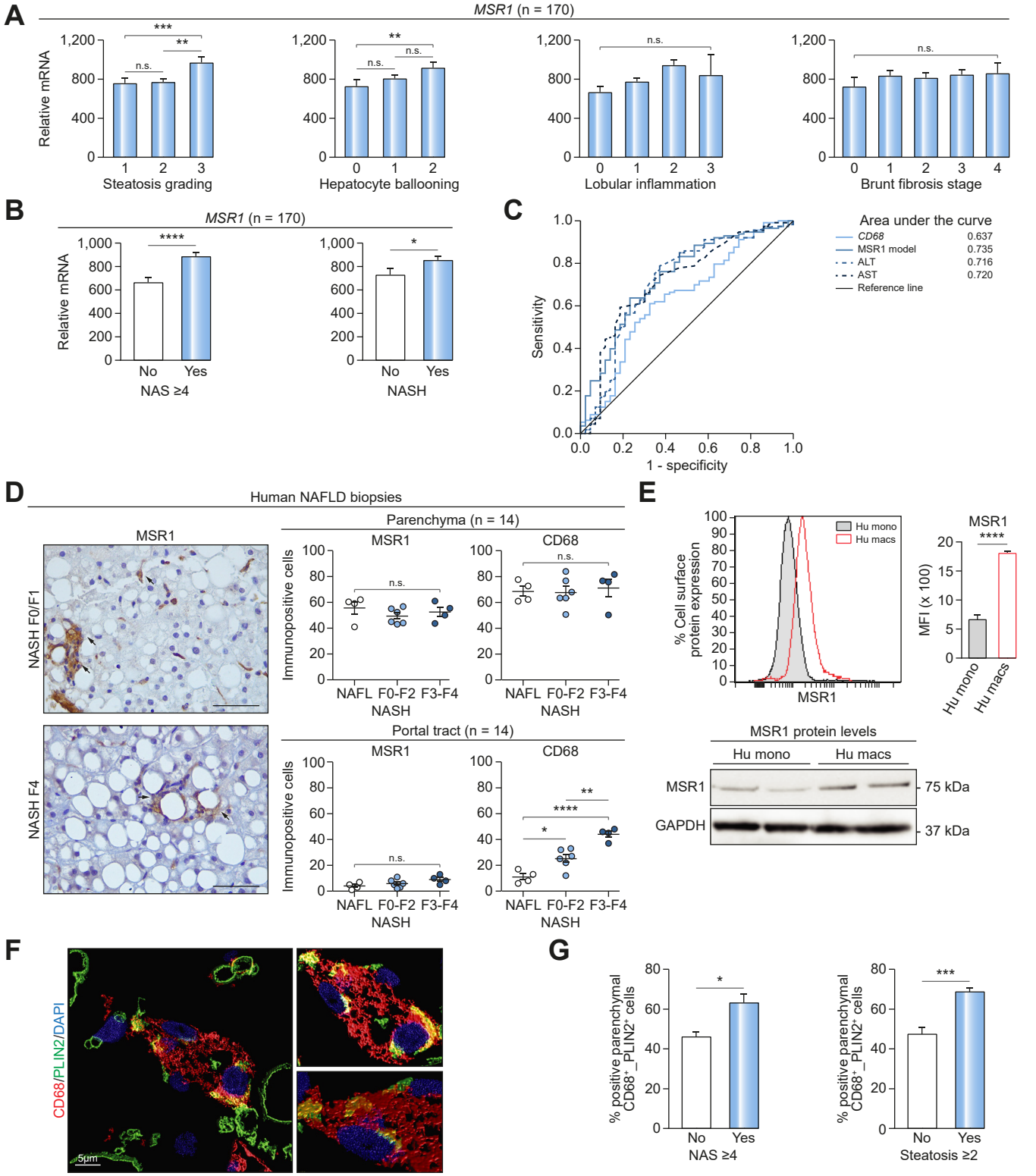

Fig. 1. MSR1 expression in human NAFLD correlates with steatosis and steatohepatitis. (A) mRNA levels of *MSR1* in a cohort of 170 histological proven NAFLD samples covering the different stages of the disease using nanoString (Mann-Whitney *U* test and Kruskal-Wallis with correction for multiple testing). (B) *MSR1* transcript in patients stratified based on NAS ≥4 and presence of NASH (Mann-Whitney *U* test). (C) Receiver-operating characteristic curve showing the binary logistic model based on *MSR1* transcript, MSR1 model, compared to other variables *CD68* transcript, ALT and AST. (D) Immunohistochemical analysis of MSR1 in human NAFLD biopsies (n = 14), arrows indicate lipogranuloma and lipid-laden macrophages. Histopathological quantification of MSR1- and CD68-immunopositive cells in the parenchyma and portal tract (NAFL n = 4; NASH F0-2 n = 6; NASH F3-4 n = 4; one-way ANOVA or Kruskal-Wallis with correction for multiple testing). (E) Differentiation of human monocytes obtained from 5 healthy volunteers towards mature macrophages. MSR1 protein expression was assessed using FACS (n = 3, unpaired Student's *t* test) and western blotting (n = 2). (F) Representative image of PLIN2+CD68+ parenchymal macrophages. Quantification was done in a cohort of 10 NAFLD samples (unpaired Student's *t* test). Data are presented as mean ± SEM (**p* <0.05, ***p* <0.01, ****p* <0.001, *****p* <0.0001, n.s., non-significant). Scale bars 100 µm. ALT, alanine aminotransferase; AST, aspartate aminotransferase; MSR1, macrophage scavenger receptor 1; NAFL, non-alcoholic fatty liver, NAFLD, non-alcoholic fatty liver; NAS, NAFLD activity score; NASH, non-alcoholic steatohepatitis.

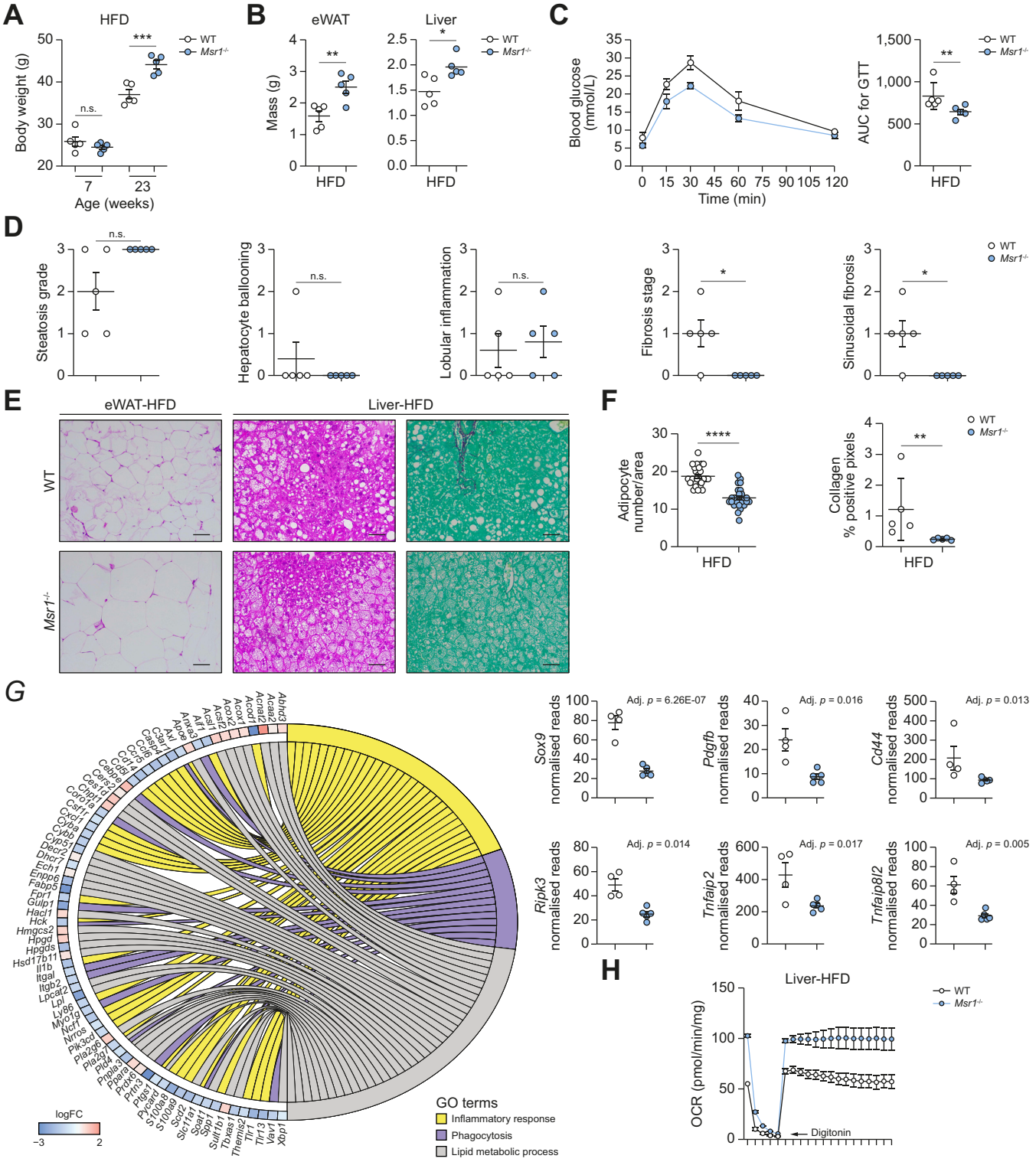

Fig. 2. Msr1 deficiency protects against HFD-associated metabolic dysregulation and liver damage. (A) Body weight of *Msr1*$^{+/+}$ (WT) and *Msr1*$^{-/-}$ male aged-matched mice fed HFD for 16 weeks (n = 5 mice/experimental group). (B) eWAT and liver mass of WT and *Msr1*$^{-/-}$ male mice fed with HFD. (C) Glucose tolerance test on overnight fasted mice during the 15th week of HFD feeding. (D) Histological characterisation of livers specimens from WT and *Msr1*$^{-/-}$ mice fed a HFD for 16 weeks. (E) Representative images of morphology of the eWAT and liver from HFD-fed WT and *Msr1*$^{-/-}$ mice. Scale bar 100 μm. (F) Quantification of the adipocyte number per area and hepatic collagen deposition of WT and *Msr1*$^{-/-}$ HFD-fed mice (n = 5 mice/experimental group). (G) RNA sequencing data comparing *Msr1*$^{-/-}$ (n = 5) with baseline WT (n = 4) HFD-fed mice. Gene Ontology enrichment analysis was performed for biological processes and selected differentially expressed genes were visualised with corrected *p* values. (H) Seahorse analysis of OCRs of liver tissue from HFD-fed WT and *Msr1*$^{-/-}$ mice (n = 4/group). Data are presented as mean ± SEM (unpaired Student's *t* test or Mann-Whitney *U* test, or one-way ANOVA with correction for multiple testing; *p* values are shown for the comparisons WT and *Msr1*$^{-/-}$; **p* <0.05, ***p* <0.01, ****p* <0.001, *****p* <0.0001, n.s., non-significant). AUC, area under the curve; eWAT, epididymal white adipose tissue; HFD, high-fat, high-cholesterol diet; Msr1, macrophage scavenger receptor 1; OCRs, oxygen consumption rates; WT, wild-type.

monoclonal rat anti-mouse Msr1 antibody (n = 8 animals, MAB1797-SP, R&Dsystems) or IgG control (n = 9 animals, MAB0061, R&D systems) at week 10 and 11 (0.25 mg antibody/animal).

Statistical analysis

Kolmogorov-Smirnov or the Shapiro-Wilk normality test, unpaired Student's *t* test or Mann-Whitney *U* test, one-way ANOVA or Kruskal-Wallis test with, respectively, Tukey's or Dunn's *post hoc* multiple comparison test or Chi-Square test were performed using IBM SPSS statistics 26 or GraphPad Prism 8.4.3. A p value <0.05 was considered significant. Binary logistic regression analysis was performed in SPSS using the backward stepwise likelihood ratio model. The model predicting high disease activity (NAFLD activity score [NAS] ≥4: NAS defined as the sum of steatosis, ballooning and lobular inflammation) was calculated as follows: MSR1_model=-1.296883 + (0.003020***MSR1*_mRNA).

For further details regarding the materials used, please refer to the CTAT table and supplementary information.

Results

MSR1 expression correlates with steatohepatitis activity in human NAFLD

To investigate the role of MSR1 in human NAFLD, we first analysed gene expression in a cohort of 170 histologically characterised human adult liver biopsies. The cohort was stratified according to histopathological disease grade and stage, *i.e.* NAFL and NASH with fibrosis ranging from F0 to F4 (Table S1). Univariate analysis indicated that the *MSR1* transcript was significantly associated with high steatosis, hepatocyte ballooning, presence of NASH and a NAS ≥4 (Fig. 1A,B and Table S2).[14] Interestingly, *CD68* mRNA, a marker for monocytes/macrophages, was only significantly associated with NAS ≥4 but not with any other clinicopathological features (Table S2). To further explore whether the *MSR1* transcript was independently associated with high disease activity, we performed binary logistic regression analysis including the clinical variables sex, BMI, age, T2DM, alanine aminotransferase (ALT) and aspartate aminotransferase (AST), together with *MSR1* and *CD68* mRNA levels. Backward stepwise likelihood ratio modelling showed that *MSR1* transcript levels predicted NAS ≥4 independently of *CD68* mRNA or other clinical variables with an AUC of 0.735 (Fig. 1C).

Histopathological analysis showed that MSR1 was predominantly expressed in resident liver macrophages, *i.e.* Kupffer cells, rather than infiltrating monocyte-derived macrophages located in the portal tract, as visualised by the MSR1 and CD68 immunostaining (Fig. 1D and Fig. S1A,B). This was confirmed by immunofluorescent double staining (Fig. S1C). While the number of infiltrating portal CD68-immunopositive cells increased with disease progression, no significant differences were found for infiltrating MSR1-positive cells (Fig. 1D). These results were supported by publicly available single-cell RNA sequencing data indicating that *MSR1* expression was mainly restricted to the Kupffer cell population whereas *CD68* was also expressed in monocyte populations (Fig. S2A,B).[15] Moreover, when differentiating monocytes from healthy individuals towards mature macrophages, we observed an increase in MSR1 protein expression (Fig. 1E). Notably, MSR1 immunopositivity was also seen in lipogranulomas and lipid-laden macrophages throughout the spectrum of NAFLD (Fig. 1D and Fig. S1A). Using the marker perilipin 2 (PLIN2) to visualise intracellular lipid droplets, immunofluorescence analysis showed that lipid droplets accumulate in Kupffer cells (Fig. 1F). Furthermore, a significant increase in parenchymal CD68+_PLIN2+ cells was observed in patients with NAFLD stratified based on NAS ≥4 or steatosis grade ≥2 (Fig. 1F).

Taken together, these human data demonstrate a positive correlation of *MSR1* transcript and protein levels with NAFLD disease activity and the occurrence of hepatic-resident lipid-laden macrophages in the presence of excessive lipids.

Msr1 deficiency protects against diet-induced metabolic dysregulation and liver damage in mice

To further investigate how MSR1 functionally contributes to the development of obesity-related NAFLD, we subjected *Msr1*$^{-/-}$ mice (n = 5) and their corresponding *Msr1*$^{+/+}$ (n = 5 WT) age-matched male counterparts to a HFD for 16 weeks. Upon HFD feeding, *Msr1*-deficient mice displayed increased total body weight, an increase in liver and epididymal white adipose tissue weight and increased food intake compared to WT (Fig. 2A,B, Fig S3A,B). Furthermore, HFD-fed *Msr1*$^{-/-}$ mice exhibited improved glucose uptake from blood, higher serum leptin, lower concentrations of circulating FFAs and enhanced fatty acid accumulation in adipocytes (Fig. 2C, Fig. S3C,D). Consistently, the adipocytes in HFD-fed *Msr1*$^{-/-}$ mice were larger than in WT mice, suggesting an increased adiposity and fat storage in the absence of *Msr1* (Fig. 2D–F). Although no murine models accurately recapitulate all histological features of human steatohepatitis, histological and transcriptomic features of liver fibrosis were clearly attenuated by *Msr1* deficiency upon HFD feeding (Fig. 2D-F). Sixteen weeks of regular diet did not result in any histological differences between the livers of WT and *Msr1*$^{-/-}$ mice (Fig. S3E), while WT mice on HFD displayed a significant higher hepatic fibrosis stage, sinusoidal fibrosis and increased collagen deposition (Fig. 2D-F, Fig. S3F) compared to the *Msr1*$^{-/-}$ mice. Next, we characterised the livers of HFD-fed WT and HFD-fed *Msr1*$^{-/-}$ mice by high-throughput RNA sequencing analysis. The analysis revealed 728 differentially expressed genes (Table S3). Gene Ontology analysis of differentially expressed genes highlighted an enrichment for genes correlating to biological processes including "innate immune response", "phagocytosis" and "lipid metabolic process" (Fig. 2G, Fig. S3G,H). HFD-fed *Msr1*$^{-/-}$ mice displayed reduced hepatic transcript expression of inflammatory cytokines (including *Axl*, *Ccl6*, *Il1b*, *Spp1*), pro-inflammatory immune cell markers (*Ccr5*, *Cd14*, *Cd44*, *S100a8*, *S100a9*), markers for hepatic stellate cell activation (*Sox9*, *Pdgfb*) and members of the *Tnfa* signalling pathway (*Ripk3*, *Tnfaip2*, *Tnfaip8l2*) when compared with WT mice (Fig. 2G). Furthermore, *Msr1*$^{-/-}$ mice on HFD showed a shift in gene expression associated with lipid metabolism, with genes including *Acox1*, *Acox2*, *Apoe*, *Ces1d*, *Hsd17b11*, *Pla2g6* and *Ppara* increasing, and genes such as *Fabp5*, *Lpcat2*, *Lpl*, *Pla2g7* and *Pnpla3* decreasing (Fig. 2G). Functionally, the measured mitochondrial oxygen consumption rate in viable liver samples of HFD-fed *Msr1*$^{-/-}$ mice was approximately 50% higher compared to that in WT mice, indicating enhanced metabolic function (Fig. 2H). Taken together, these results demonstrate that *Msr1* deficiency increases body weight but protects against features of the metabolic syndrome, including liver inflammation and fibrosis, while modulating hepatic lipid metabolism.

Msr1 deficiency prevents formation of pro-inflammatory foamy macrophages *in vivo*

Next, we asked whether the lipid-laden environment is a proximal stimulus leading to Msr1-mediated inflammation in the liver and adipose tissue, which may explain the observed metabolic dysfunction. In agreement with our human data, histopathological analysis of the liver and adipose tissue from HFD-fed *Msr1* $^{-/-}$ mice showed no hepatic lipogranuloma and very few foamy macrophages compared to their WT counterparts, demonstrated by F4/80 immunostaining (Fig. 3A). Moreover, *Msr1*$^{-/-}$ mice displayed lower Il6 and Tnfα serum levels and reduced *Tnfa* and *Il6* gene expression in the liver and epididymal white adipose tissue (Fig. 3B-D). Furthermore, *Msr1* deficiency impaired pro-inflammatory activation of isolated adipose tissue macrophages and hepatic-associated macrophages as shown by lower gene transcripts of *Tnfa* and *Il6* (Fig. 3E-G). Altogether, these results show that Msr1 mediates HFD-induced hepatic and adipose tissue inflammation and facilitates macrophage activation towards a pro-inflammatory phenotype.

Triggering of Msr1 by lipids induces JNK-mediated pro-inflammatory activation of macrophages

We next investigated the underlying mechanism of Msr1-mediated lipid-induced inflammation. We reasoned that Msr1 is directly responsible for lipid uptake in macrophages, leading to an inflammatory response independent from other cell types. In this regard, we measured the uptake of SFA (palmitic acid) and non-SFA (oleic acid) in *Msr1*$^{-/-}$ and WT BMDMs by quantifying Oil-red-O staining using confocal microscopy (Fig. 4A-C, Fig. S4A). The analysis revealed that Msr1 facilitates the uptake of both SFA and non-SFA but only SFA induced enhanced levels of *Tnfa* and *Il6* transcripts in BMDMs (Fig. 4D). Furthermore, blocking the Msr1 receptor with a monoclonal antibody reduced the expression of *Tnfa* and *Il6*, and reduced the phosphorylation of JNK in response to SFA treatment (Fig. 4E,F). In line with these data, pharmacological inhibition of JNK phosphorylation abrogated the induction of *Tnfa* and *Il6* pro-inflammatory gene expression upon SFA treatment (Fig. S4B). Similarly, using primary *Msr1*$^{-/-}$ hepatic macrophages or WT ones treated with

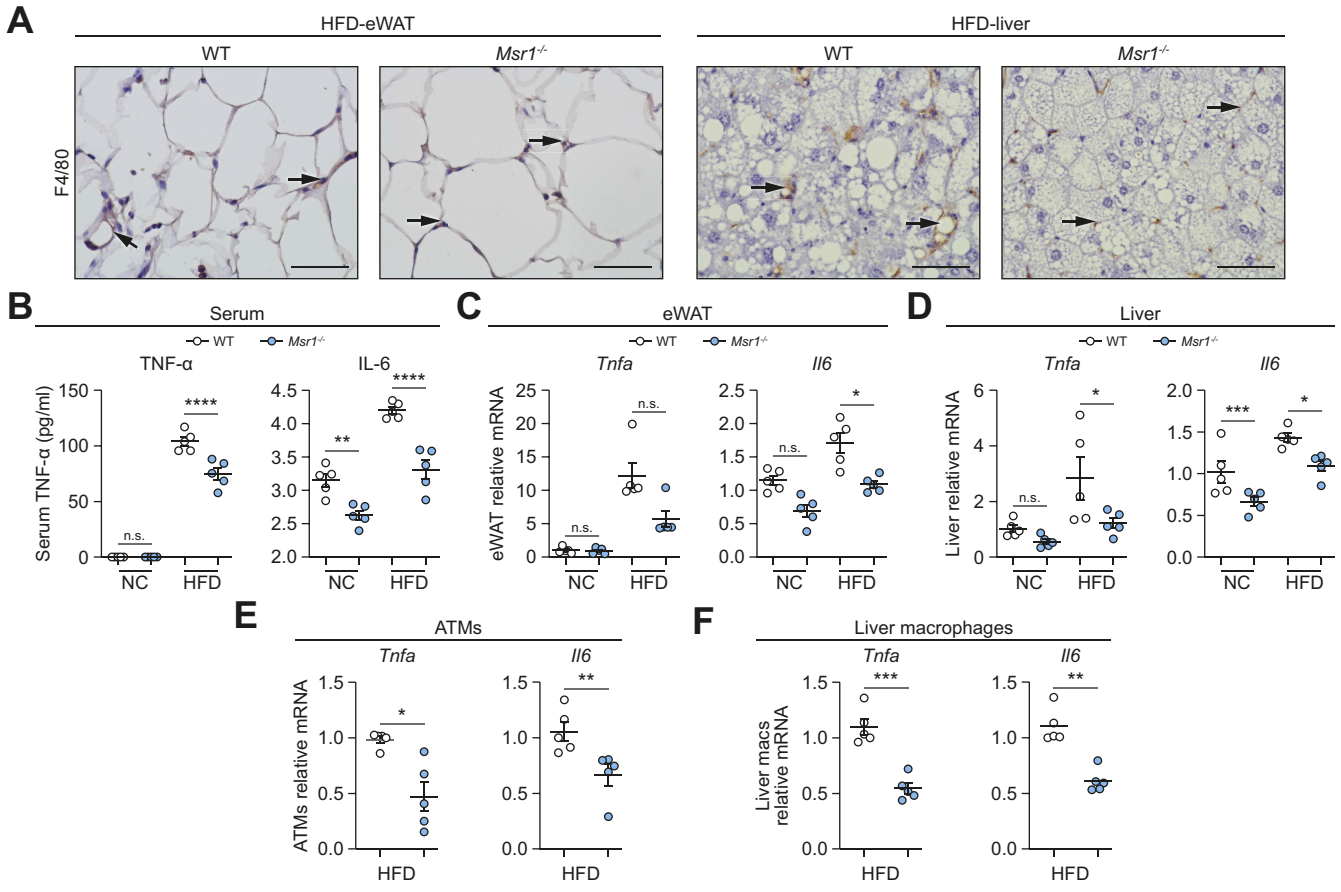

Fig. 3. Msr1 mediates HFD-induced adipose tissue and hepatic inflammation and facilitates macrophage activation towards a pro-inflammatory phenotype. (A) Representative images for F4/80 immunostainings in eWAT and liver (scale bars 100 μm) from WT and *Msr1*$^{-/-}$ HFD-fed mice (n = 5/experimental group). Arrows indicate immunopositive cells. (B) Serum levels of Tnfa and Il-6 in NC- and HFD-fed mice (n = 5/ group). (C,D) Quantification of mRNA levels of *Tnfa, Il6* inflammation markers in the eWAT and liver of NC- and HFD-fed mice (n = 5/group). (E,F) Real-time PCR analysis for markers of inflammation in isolated F4/80^{+} adipose tissue (ATMs) and liver macrophages (n = 5 mice/group). Data are presented as mean ± SEM (unpaired Student's *t* test or Mann-Whitney *U* test, or one-way ANOVA or Kruskal-Wallis with correction for multiple testing; *p* values are shown for the comparisons WT and *Msr1*$^{-/-}$; *p< 0.05, ***p* <0.01, ****p* <0.001, *****p* <0.0001, n.s., non-significant). ATMs, adipose tissue-associated macrophages; eWAT, epididymal white adipose tissue; HFD, high-fat, high-cholesterol diet; Msr1, macrophage scavenger receptor 1; NC, normal chow; WT, wild-type.

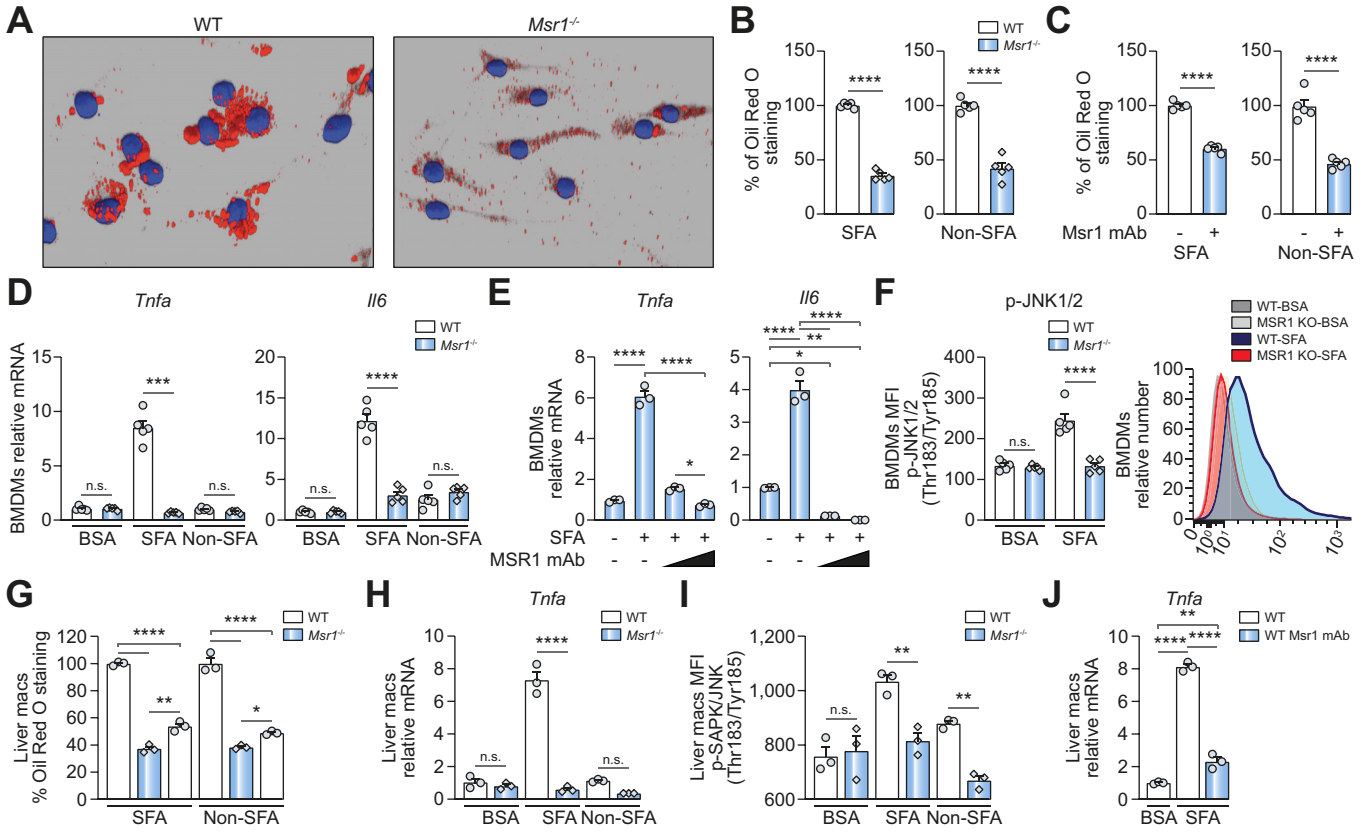

Fig. 4. Msr1 regulates JNK-mediated lipid-induced pro-inflammatory activation of macrophages. (A) Representative image of lipid uptake (mixture of 1 mM palmitic acid [an SFA] and 2 mM oleic acid [a non-SFA]) by WT and *Msr1*$^{-/-}$ BMDMs visualised by Oil-red-O staining using confocal microscopy (n = 3). (B,C) Quantification of SFA (palmitic acid 1 mM) and non-SFA (oleic acid 2 mM) uptake in WT and *Msr1*$^{-/-}$ BMDMs, or WT BMDMs pre-treated with or without anti-Msr1 antibody (n = 5). Data are normalised to the average of the WT BMDM group. (D) Real-time PCR analysis for *Tnfa* and *Il6* in WT and *Msr1*$^{-/-}$ BMDMs stimulated or not either with SFA, non-SFA or BSA control for 6 hours. (E) Real-time PCR analysis of BMDMs with or without SFA stimulation that were treated with 10 or 25 μg/ml anti-Msr1 monoclonal antibody for 6 hours. (F) Flow cytometry analysis and quantification of JNK1/2 phosphorylation in WT and *Msr1*$^{-/-}$ BMDMs stimulated with SFA or BSA control. (G) Quantification of SFA and non-SFA uptake in WT and *Msr1*$^{-/-}$ primary liver macrophages (n = 3). Data are normalised to the average of the WT BMDM group. (H) Real-time PCR analysis and (I) flow cytometry analysis of phospho-JNK (Thr183/Tyr185) in WT and *Msr1*$^{-/-}$ primary liver macrophages treated either with control BSA or SFA or non-SFA for 6 hours (n = 3). (J) Real-time PCR analysis of WT primary liver macrophages treated with or without monoclonal anti-Msr1 antibody (n = 3). Data are shown as mean ± SEM (unpaired Student's *t* test or one-way ANOVA/Kruskal-Wallis with correction for multiple testing; for panels D and F-I the *p* values are shown only for grouped comparisons per experimental condition; **p* <0.05, ***p* <0.01, ****p* <0.001, *****p* <0.0001). BMDM(s), bone marrow-derived macrophages; KO, knockout; mAb, monoclonal antibody; MSR1, macrophage scavenger receptor 1; SFA, saturated fatty acid; WT, wild-type.

monoclonal antibody resulted in reduced lipid uptake, reduced expression of *Tnfa* and reduced JNK phosphorylation (Fig. 4G-J). To extend these findings, we co-cultured Hepa1-6 cells with BMDMs or primary hepatocytes with hepatic macrophages, which resulted in a comparable response (Fig. S5A–E). These data indicate that SFA-induced triggering of Msr1 regulates JNK-mediated pro-inflammatory activation of macrophages in the absence of lipopolysaccharide.

Therapeutic inhibition of MSR1 reduces the release of TNFA

To investigate the therapeutic potential of targeting MSR1 in the treatment of NAFLD, we applied an antibody-based intervention using NAFLD mouse models and *ex vivo* human liver slices. WT mice were fed a HFD for 12 weeks and were administered 2 doses of monoclonal rat anti-mouse Msr1 antibody (n = 8 animals) or isotype-matched IgG control (n = 9 animals) at week 10 and 11 by intravenous injection. Antibody treatment did not result in any weight difference or changes in glucose or insulin levels at week 12 (Fig. S6). Notably, histological assessment did show reduced hepatic fibrosis and sinusoidal/peri-cellular fibrosis in anti-Msr1-treated mice compared to the IgG control mice, while steatosis grade, hepatocyte ballooning and lobular inflammation remained unchanged (Fig. 5A,B). In addition, F4/80 immunostaining showed a reduction in occurrence of hepatic foamy macrophages and lipogranulomas upon treatment, which translated into reduced surface area positivity of F4/80-positive cells (Fig. 5B,C). Furthermore, treated animals showed reduced expression of *Tnfa* transcript in liver samples and isolated hepatic macrophages (Fig. 5D–E).

To further investigate whether inhibition of MSR1 prevents the formation of foamy macrophages and release of TNFA in humans, we collected human liver slices with normal morphology from 2 different patients (2 biological replicates per condition for each patient sample). The samples were incubated with a polyclonal anti-human MSR1 antibody prior to culturing them with a mixture of oleic acid (2 mM) and palmitic acid (1 mM) combined with anti-MSR1 antibody for 16 h (Fig. 5F). Treatment with the antibody reduced the surface area positivity

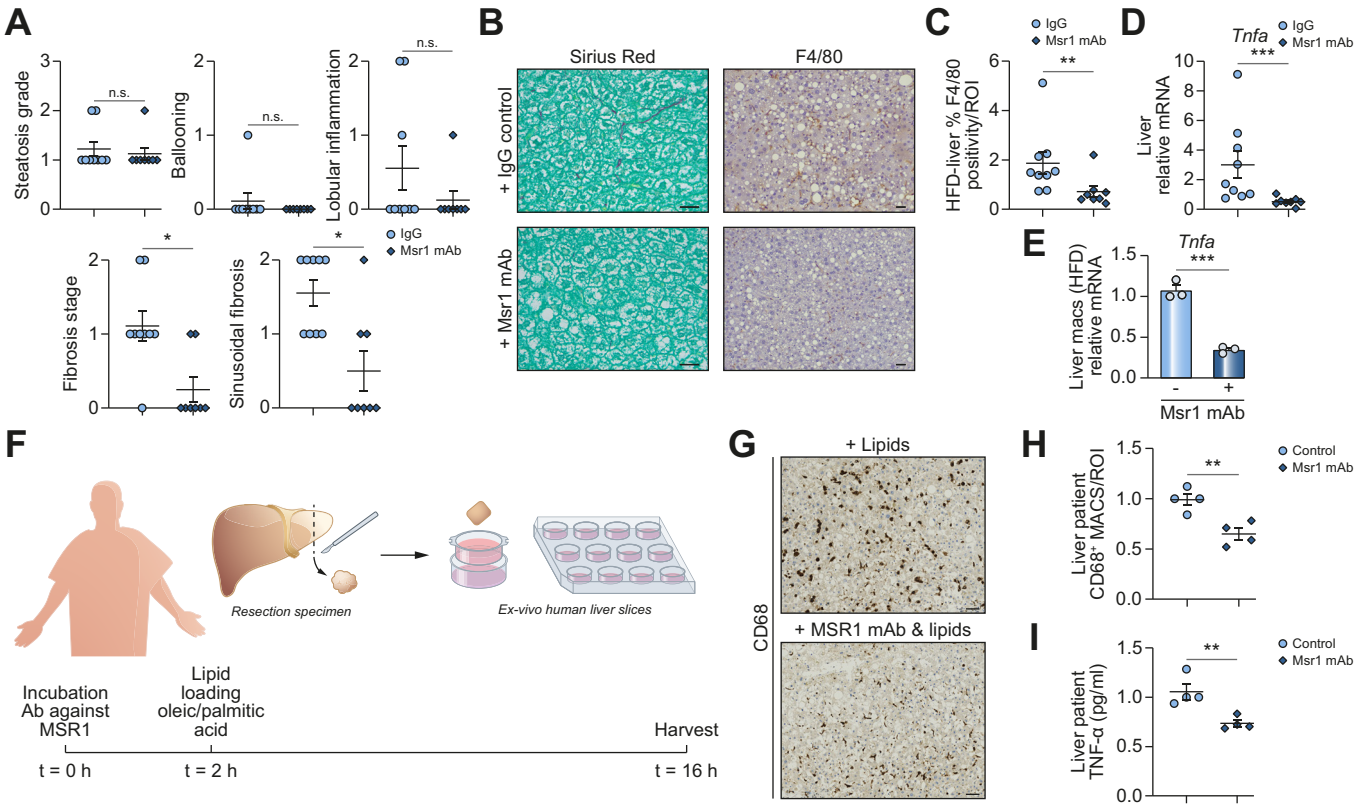

Fig. 5. Therapeutic inhibition of MSR1 prevents formation of pro-inflammatory foamy macrophages. (A) Histological characterisation of liver specimens from WT male mice fed a HFD for 12 weeks and treated with anti-Msr1 antibody (n = 8) or IgG control (n = 9) at week 10 and 11. (B) Representative images of morphology of HFD-fed animals treated with anti-Msr1 antibody or IgG control. (C) Quantification of F4/80 staining from treated animals presented as percentage pixel positivity of the ROI. (D,E) Real-time PCR analysis for *Tnfa* transcript in liver samples and isolated hepatic macrophages from HFD-fed animals treated with anti-Msr1 antibody (n = 8) or IgG control (n = 9). Isolated primary liver macrophages were pooled together before real-time PCR analysis (n = 3). (F) Schematic overview of antibody-based treatment of *ex vivo* lipid-loaded human liver slices. Samples were loaded with a combination of oleic acid (2 mM) and palmitic acid (1 mM). (G) Immunohistochemical staining for CD68 on human lipid-loaded liver slices treated with or without anti-MSR1 antibody. (H) Quantification of CD68 staining presented as percentage pixel positivity of the ROI. Normalisation was done to untreated reference. (I) TNF-α ELISA from human liver slices treated with lipids or anti-MSR1-antibody+lipids. Data are presented as mean ± SEM (unpaired Student's *t* test or Mann-Whitney *U* test; $^{*}p$ <0.05, $^{**}p$ <0.01, $^{***}p$ <0.001). Scale bars 50 μm. HFD, high-fat, high-cholesterol diet; mAb, monoclonal antibody; MSR1, macrophage scavenger receptor 1; ROI, region of interest; WT, wild-type.

of Kupffer cells as shown by CD68 immunostaining (Fig. 5G,H). Moreover, lipid-induced release of TNF-α into the culture medium was reduced upon anti-MSR1 antibody treatment (Fig. 5I). Overall, our *in vivo* and *ex vivo* results show that therapeutic inhibition of MSR1 prevents the formation of foamy macrophages and the release of TNF-α.

Relevance of polymorphisms in *MSR1* region to NAFLD and metabolic traits

Next, we asked whether genetic variants in *MSR1* are associated with susceptibility to NAFLD and if there is an association with transcriptional regulatory mechanisms controlling *MSR1* expression. Using previously published genomics data encompassing a cohort of 1,483 European Caucasian patients with histologically proven NAFLD and 17,781 European general-population controls,[13] we identified 4 single nucleotide polymorphisms (SNPs) in or around the *MSR1* locus with *p* values $<5^{*}10^{-4}$, with rs41505344 as the most significant ($p = 1.64^{*}10^{-4}$) (Fig. 6A and Table S4). Quantitative trait analysis for rs41505344 in 430,101 patients enrolled in the UK Biobank showed a significant correlation with serum triglycerides and AST levels, even after adjustment for age, sex, BMI, centre, batch and the first 10 principal components (Table 1).

Our human data indicated that MSR1 is expressed in the liver on mature endogenous macrophages rather than on infiltrating monocyte-derived macrophages. To unravel transcriptional regulatory mechanisms of *MSR1*, we used publicly available RNA sequencing data comparing human monocytes with differentiated macrophages, which identified 1,208 differentially expressed genes, with *MSR1* mRNA expression increased in the macrophage population.[16] By motif enrichment analysis using iRegulon, we identified 8 differentially expressed transcription factors, upregulated in human macrophages compared to monocytes, that are predicted to regulate the expression of *MSR1*: *BHLHE41*, *ETV5*, *HMGN3*, *MAF*, *MITF*, *NR1H3*, *THRA* and *ZNF562* (Fig. 6B, Table S5). To verify whether these transcription factors bind any regulatory regions near the *MSR1* gene, and in particular the rs41505344 SNP locus, we investigated chromatin-immunoprecipitation sequencing data for these proteins. *MITF*, *MAF*, *THRA* and *NR1H3* proved to bind in the vicinity of the rs41505344 locus, suggesting an indirect role for the SNP in the transcriptional regulation of *MSR1* (Fig. 6C). When assessing the rs41505344 genotype in our nanoString cohort, a significant

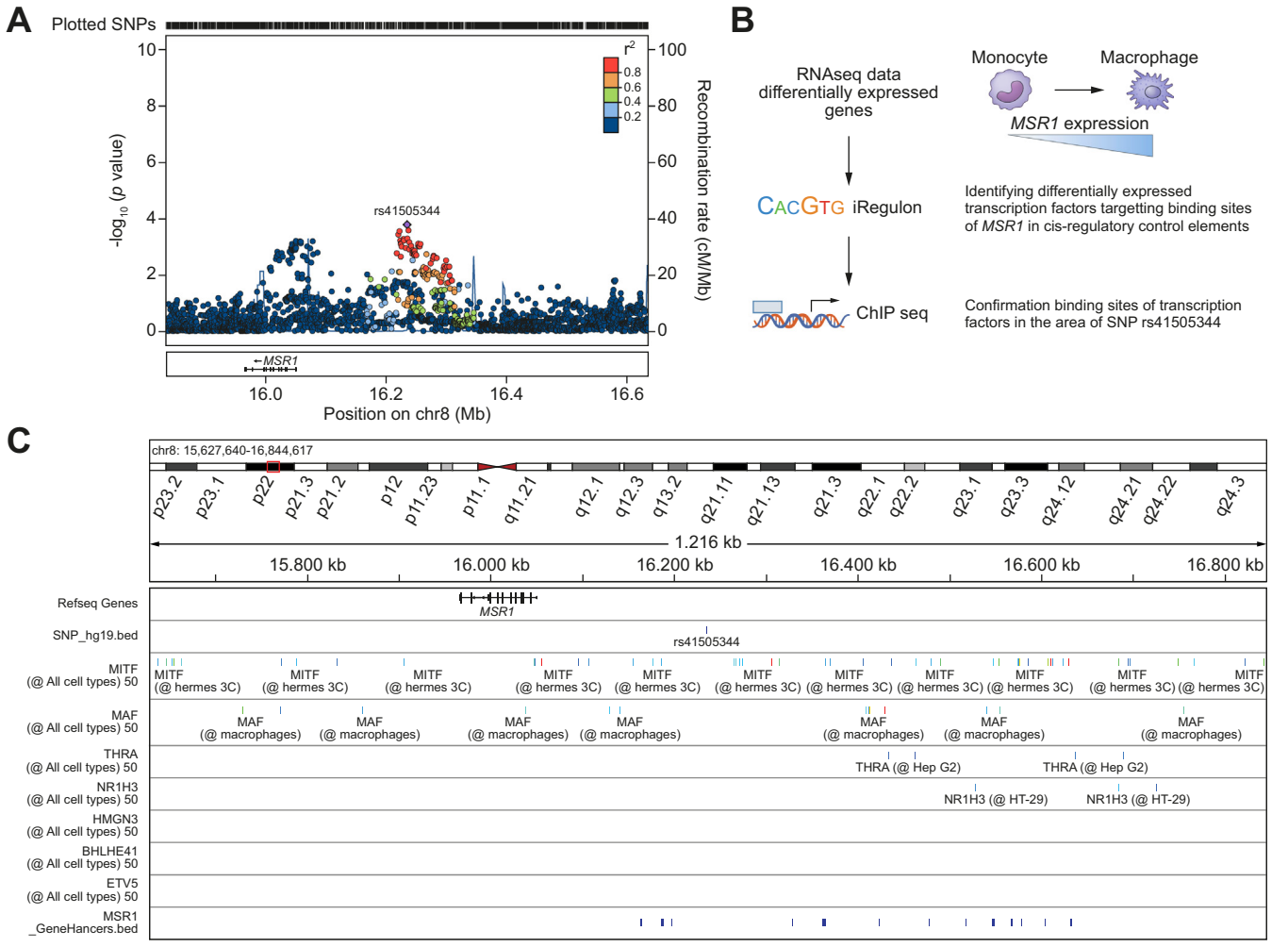

Fig. 6. Regulatory mechanisms of *MSR1* expression in human NAFLD. (A) Locus plot showing *MSR1* rs41505344 SNP based on case-control analysis comparing 1,483 histologically characterised NAFLD samples with 17,781 matched population controls. (B) Schematic overview of the workflow used to identify transcriptional regulatory mechanisms of *MSR1* from publicly available RNA sequencing data, comparing human monocytes with differentiated macrophages.[16] (C) Visualisation of chromatin-immunoprecipitation sequencing data around *MSR1* rs41505344 SNP of the predicted transcription factors that are differentially expressed in the RNA sequencing data as identified by iRegulon. Bottom row indicates known transcriptional regulatory regions of *MSR1*. MSR1, macrophage scavenger receptor 1; NAFLD, non-alcoholic fatty liver disease; SNP, single nucleotide polymorphism.

increase in *MSR1* transcript levels was observed in patients carrying the SNP (Fig. S7).

Taken together, these results suggest that the frequency of variants potentially affecting *MSR1* expression during monocyte-macrophage differentiation, which could influence features of obesity-related diseases, is increased in patients with NAFLD.

Discussion

In this study, we provide evidence that MSR1 is important for the uptake of lipids in macrophages, leading to an inflammatory response and metabolic changes throughout the body. In a setting of lipid overload, MSR1 deficiency not only led to reduced hepatic inflammation and changes in hepatic lipid metabolism but it also reduced circulating fatty acids, increased lipid storage in the adipose tissue and improved glucose tolerance, highlighting the importance of the liver-adipose tissue axis in NAFLD and the metabolic syndrome.[17] Our data demonstrated that MSR1 was expressed in tissue-resident macrophages, *i.e.* Kupffer cells, rather than in infiltrating monocytes, and that its expression increases as human monocytes differentiate towards mature macrophages.[16,18] The association between *MSR1* mRNA and disease activity in our study would suggest that there is an ongoing differentiation from infiltrating monocytes towards macrophages during NASH. Although portal inflammation is associated with advanced NAFLD, lobular inflammation has been reported to predict fibrosis progression in human NAFLD, suggesting that disease progression is driven by tissue-resident macrophages rather than infiltrating monocytes.[19] Our results support this as *Msr1* deficiency in HFD-fed mice tempered the lipid-induced inflammatory response in the liver, by reducing the expression of *Axl*, *Il1b*, *S100a8/a9* and *Spp1* but also *Cd44*. Cd44 expression has been associated with NASH in human and mouse, and is crucial for homing of monocytes into the damaged liver, suggesting that lipid accumulation in tissue-resident macrophages via MSR1 is a trigger to recruit immune cells.[20] This is in line with a previous study reporting that Kupffer cell depletion by clodronate liposomes reduces infiltration of inflammatory cells, mainly monocytes, into the livers of mice on a 22-week

Table 1. Correlation of rs41505344 SNP with clinical features in participants from the UK Biobank (N = 430,101).

Characteristic	Total	rs41505344_*MSR1*				Unadjusted	Adjusted for age, sex, BMI, PC 1-10, centre and batch		
		GG	GA	AA			Inverse normal rank transformation		
	Value (range)*	Value (range)*	Value (range)*	Value (range)*	*p* value	*p* value	Beta	CI
n	430,101	344,142	81,079	4,880				
Age, years, mean ± SD	56.8±8.03 (39–73)	56.8±8.03 (39–72)	56.8±8.02 (39–73)	56.7±8.06 (40–70)	0.80			
BMI, mean ± SD	27.4±4.76 (12.1–74.7)	27.4±4.77 (12.6–68.4)	27.4±4.75 (12.1–74.7)	27.3±4.81 (16.2–54.5)	0.02			
Male, n (%)	196,727 (45.7)	157,394 (45.7)	37,080 (45.7)	2,253 (46.2)	0.80			
ALT, U/L	23.5±14.1(3.01–495)	23.6±14.1 (3.1–495)	23.5±14.3 (3.01–472)	23.3±13.1 (3.82–286)	0.01	0.063	–0.0060	
AST, U/L	26.2±10.6 (3.3–947)	26.2±10.5 (3.3–947)	26.2±11 (3.3–711)	26±9.72 (8.4–227)	8.29E–04	0.003	–0.010	
Glucose, mM	5.12±1.21 (1–36.8)	5.12±1.2 (1.1–36.8)	5.12±1.23 (1–32.7)	5.12±1.18 (1.8–22.3)	0.76	0.41	0.003	
Cholesterol, mM	5.71±1.14 (0.601–15.5)	5.71±1.14 (0.601–15.5)	5.71±1.14 (1.71–13.3)	5.68±1.13 (2.39–12.3)	0.16	0.12	–0.005	
LDL, mM	3.57±0.87 (0.266–9.8)	3.57±0.87 (0.266–9.8)	3.57±0.868 (0.751–9.61)	3.55±0.862 (1.22–7.64)	0.16	0.15	–0.0051	
HDL, mM	1.45±0.382 (0.219–4.4)	1.45±0.382 (0.226–4.4)	1.46±0.382 (0.219–4.13)	1.45±0.38 (0.628–3.22)	0.03	0.071	0.006	
Triglycerides, mM	1.75±1.02 (0.231–11.3)	1.76±1.03 (0.233–11.3)	1.74±1.02 (0.231–11.3)	1.72±1 (0.375–11)	8.27E–07	3.55E–06	–0.015	
Chronic liver disease, n (%)	6,024 (1.401)	4,807 (1.397)	1,161 (1.432)	56 (1.148)	0.98	0.92	1.003	0.946–1.06
All-cause cirrhosis, n (%)	1,709 (0.397)	1,349 (0.392)	344 (0.424)	16 (0.328)	0.40	0.37	1.051	0.943–1.17

ALT, alanine aminotransferase; AST, aspartate aminotransferase; PC, principal component; SNP, single nucleotide polymorphism.
*Values in brackets denote range for continuous variables or (%) for categorical variables.

choline-deficient l-amino acid-defined diet.[21] Furthermore, our results showed that the absence of Msr1 induced a change in hepatic expression of genes associated with lipid metabolism, including an increase in *Ppara*, with concordantly increased mitochondrial oxygen consumption and ameliorated glucose tolerance in HFD-fed mice. Peroxisome proliferator-activated receptors (PPAR) are nuclear receptors that play key roles in metabolic homeostasis and inflammation.[22] Selective Kupffer cell depletion has been reported to activate Ppara signalling in hepatocytes while resulting in overall reduced levels of hepatic triglycerides in mice fed a 45%-HFD.[23] Furthermore, hepatocyte-restricted *Ppara* deletion in mice impaired liver lipid metabolism, leading to increased plasma FFAs.[24] In human adult patients with non-cirrhotic NASH, the pan-PPAR agonist lanifibranor induced NASH resolution after 24 weeks of treatment in a phase IIb randomised, placebo-controlled, double-blind study.[25] Taken together, the effects of Msr1 deficiency on liver metabolism, triglycerides and circulating FFAs observed in this study could in part be explained by altered Ppara signalling in the liver.

This study showed that MSR1 can facilitate the uptake of SFAs, such as palmitic acid, as well as non-SFAs, such as oleic acid, independently of other receptors. Yet, only SFAs could induce the release of TNFα through phosphorylation of JNK in macrophages, which is in line with previous reports.[7–9] In our *Msr1*$^{-/-}$ HFD-fed mice, we observed lower hepatic *Tnfa* expression as well as lower serum Tnfα. Furthermore, therapeutic blocking of MSR1 *in vivo* or *ex vivo* reduced foamy macrophage formation and the release of TNFα. TNFα has a pleiotropic effect as it can sensitise hepatocytes to apoptosis and it can stimulate hepatic lipid synthesis while reducing *Ppara* expression.[26,27] Furthermore, Tnfα affects glucose homeostasis in adipocytes and promotes lipolysis in cultured adipocytes, which could explain the obese phenotype in our *Msr1*$^{-/-}$ HFD-fed mice.[28]

Although current efforts to develop drug therapies for NAFLD primarily focus on ameliorating the specific histological features of the disease (*i.e.* steatohepatitis or fibrosis), it is important to remember that NAFLD is part of a multi-system metabolic disease state and so agents that offer more broad metabolic or cardiovascular benefits would be highly attractive. Our data indicate that by targeting MSR1, one would not only reduce lipid-induced inflammation in the liver but also improve dyslipidaemia and increase lipid storage in adipocytes. In addition, we demonstrated the feasibility of using targeted monoclonal antibody therapy to treat NASH by reducing hepatic inflammation. Moreover, we found some evidence that the genetic variant rs41505344 in *MSR1* was associated with serum triglycerides and ALT in a large cohort of over 400,000 patients. Though the SNP in *MSR1* was not strongly associated with susceptibility to NAFLD, we found that several transcription factors regulating the expression of *MSR1* bound in the locus and that the SNP was associated with changes in *MSR1* transcript levels, indicating a role for rs41505344 during macrophage differentiation.

This study has several limitations. We used a global knock-out mouse model and focused on the early phases of NAFLD by using a relatively short-term diet of 16 weeks. To further investigate the liver-adipose tissue axis, a Kupffer cell-specific *Msr1* knock-out or a conditional *Msr1* knock-out mouse model challenged with a long-term diet would provide more information on advanced NAFLD. Furthermore, we mainly explored the role of SFAs in macrophages, but this does not exclude that exosomes or oxidised LDL can have an additive effect on the inflammatory

response, nor have we explored the synergetic function of other scavenger receptors such as CD36 or TREM2.

This study showed that the scavenger receptor MSR1, as part of the innate immune system, is a critical sensor for lipid homeostasis, highlighting the importance of the liver-adipose tissue axis. With the prevalence of obesity increasing globally, it is crucial that we understand how our immune system reacts when challenged with over-nutrition. Understanding and therapeutically influencing macrophage immunometabolism could help us treat features of the metabolic syndrome, such as dyslipidaemia, NAFLD and T2DM.

Abbreviations

ALT, alanine aminotransferase; AST, aspartate aminotransferase; BMDMs, bone marrow-derived macrophages; FFAs, free fatty acids; HFD, high-fat, high-cholesterol diet; MSR1, macrophage scavenger receptor 1; NAFL, non-alcoholic fatty liver; NAFLD, non-alcoholic fatty liver; NAS, NAFLD activity score; NASH, non-alcoholic steatohepatitis; PPAR, peroxisome proliferator-activated receptors; SFA, saturated fatty acid; SNPs, single nucleotide polymorphisms; T2DM, type 2 diabetes mellitus; WT, wild-type.

Financial support

This study has been supported by the EPoS (Elucidating Pathways of Steatohepatitis) consortium funded by the Horizon 2020 Framework Program of the European Union under Grant Agreement 634413, the LITMUS (Liver Investigation: Testing Marker Utility in Steatohepatitis) consortium funded by the Innovative Medicines Initiative (IMI2) Program of the European Union under Grant Agreement 777377, which receives funding from the EU Horizon 2020 programme and EFPIA, and the Newcastle NIHR Biomedical Research Centre (to QMA), the Newcastle University start-up funding and the Wellcome Trust Investigator Award (215542/Z/19/Z) (to MT), Knut och Alice Wallenberg Foundation Wallenberg Centre for molecular and translational medicine, University of Gothenburg, Sweden and Åke Wirbergs Research funding #M18-0121 (to AH), Cancerfonfen # 19 0352 Pj (2020-2022) (to AH), the Belgian Federal Science Policy Office (Interuniversity Attraction Poles Program) grant Network P7/83-HEPRO2 (to TR), Rosetrees Trust (to NML), Flemish Cancer Society Kom op tegen Kanker, and Belgian Cancer Society Stichting tegen Kanker (to J.W).

Conflict of interest

The authors have no potential conflicts (financial, professional or personal) directly relevant to the manuscript.

Please refer to the accompanying ICMJE disclosure forms for further details.

Authors' contributions

OG and AH conceived the study. Study design, manuscript drafting and funding: AH, OG, MT and QMA. Manuscript preparation: AH, OG, SKP, MT, QMA. *In vivo* experiments: AH, SKP, OBG and NML. *In vitro* experiments: AH, OG and SKP. Human *ex vivo* experiments: OG, MVH, TR. Histopathology: OG, MVH, TR and DT. Nanostring analysis: OG. Bioinformatics: OG and JW. GWAS analysis: RD, HJC, AKD. eQTL UKBiobank data: RMM, OJ, SR. All authors contributed to data collection and interpretation, and critically revised the manuscript for intellectual content.

Data availability statement

To review GEO accession GSE163471:

Go to https://www.ncbi.nlm.nih.gov/geo/query/acc.cgi?acc=GSE163471.

Acknowledgments

The authors would like to thank the Newcastle Bioimaging Unit, the Newcastle University Genomics Core Facility, the Newcastle NanoString Core Facility and the Newcastle Molecular Pathology Node Proximity Laboratory for their technical support.

Supplementary data

Supplementary data to this article can be found online at https://doi.org/10.1016/j.jhep.2021.12.012.

References

Author names in bold designate shared co-first authorship

[1] **Anstee QM**, **Reeves HL**, **Kotsiliti E**, Govaere O, Heikenwalder M. From NASH to HCC: current concepts and future challenges. Nat Rev Gastroenterol Hepatol 2019;16:411–428.
[2] Govaere O, Cockell S, Tiniakos D, Queen R, Younes R, Vacca M, et al. Transcriptomic profiling across the nonalcoholic fatty liver disease spectrum reveals gene signatures for steatohepatitis and fibrosis. Sci Transl Med 2020;12.
[3] Krenkel O, Puengel T, Govaere O, Abdallah AT, Mossanen JC, Kohlhepp M, et al. Therapeutic inhibition of inflammatory monocyte recruitment reduces steatohepatitis and liver fibrosis. Hepatology 2018;67:1270–1283.
[4] Kazankov K, Jorgensen SMD, Thomsen KL, Moller HJ, Vilstrup H, George J, et al. The role of macrophages in nonalcoholic fatty liver disease and nonalcoholic steatohepatitis. Nat Rev Gastroenterol Hepatol 2019;16:145–159.
[5] Tiniakos DG, Vos MB, Brunt EM. Nonalcoholic fatty liver disease: pathology and pathogenesis. Annu Rev Pathol 2010;5:145–171.
[6] Luukkonen PK, Sadevirta S, Zhou Y, Kayser B, Ali A, Ahonen L, et al. Saturated fat is more metabolically harmful for the human liver than unsaturated fat or simple sugars. Diabetes Care 2018;41:1732–1739.
[7] Holzer RG, Park EJ, Li N, Tran H, Chen M, Choi C, et al. Saturated fatty acids induce c-Src clustering within membrane subdomains, leading to JNK activation. Cell 2011;147:173–184.
[8] Lancaster GI, Langley KG, Berglund NA, Kammoun HL, Reibe S, Estevez E, et al. Evidence that TLR4 is not a receptor for saturated fatty acids but mediates lipid-induced inflammation by reprogramming macrophage metabolism. Cell Metab 2018;27:1096–1110 e1095.
[9] Guo M, Hartlova A, Gierlinski M, Prescott A, Castellvi J, Losa JH, et al. Triggering MSR1 promotes JNK-mediated inflammation in IL-4-activated macrophages. EMBO J 2019;38.
[10] Manning-Tobin JJ, Moore KJ, Seimon TA, Bell SA, Sharuk M, Alvarez-Leite JI, et al. Loss of SR-A and CD36 activity reduces atherosclerotic lesion complexity without abrogating foam cell formation in hyperlipidemic mice. Arterioscler Thromb Vasc Biol 2009;29:19–26.
[11] Bieghs V, Wouters K, van Gorp PJ, Gijbels MJ, de Winther MP, Binder CJ, et al. Role of scavenger receptor A and CD36 in diet-induced nonalcoholic steatohepatitis in hyperlipidemic mice. Gastroenterology 2010;138:2477–2486. 2486 e2471-2473.
[12] Hardy T, Wonders K, Younes R, Aithal GP, Aller R, Allison M, et al. The European NAFLD Registry: a real-world longitudinal cohort study of nonalcoholic fatty liver disease. Contemp Clin Trials 2020;98:106175.
[13] Anstee QM, Darlay R, Cockell S, Meroni M, Govaere O, Tiniakos D, et al. Genome-wide association study of non-alcoholic fatty liver and steatohepatitis in a histologically characterised cohort. J Hepatol 2020;73:505–515.
[14] Kleiner DE, Brunt EM, Van Natta M, Behling C, Contos MJ, Cummings OW, et al. Design and validation of a histological scoring system for nonalcoholic fatty liver disease. Hepatology 2005;41:1313–1321.
[15] Ramachandran P, Dobie R, Wilson-Kanamori JR, Dora EF, Henderson BEP, Luu NT, et al. Resolving the fibrotic niche of human liver cirrhosis at single-cell level. Nature 2019;575:512–518.
[16] Dong C, Zhao G, Zhong M, Yue Y, Wu L, Xiong S. RNA sequencing and transcriptomal analysis of human monocyte to macrophage differentiation. Gene 2013;519:279–287.

[17] Gastaldelli A, Cusi K. From NASH to diabetes and from diabetes to NASH: mechanisms and treatment options. JHEP Rep 2019;1:312–328.
[18] Govaere O, Cockell S, Van Haele M, Wouters J, Van Delm W, Van den Eynde K, et al. High-throughput sequencing identifies aetiology-dependent differences in ductular reaction in human chronic liver disease. J Pathol 2019;248:66–76.
[19] Brunt EM, Kleiner DE, Wilson LA, Unalp A, Behling CE, Lavine JE, et al. Portal chronic inflammation in nonalcoholic fatty liver disease (NAFLD): a histologic marker of advanced NAFLD-Clinicopathologic correlations from the nonalcoholic steatohepatitis clinical research network. Hepatology 2009;49:809–820.
[20] Patouraux S, Rousseau D, Bonnafous S, Lebeaupin C, Luci C, Canivet CM, et al. CD44 is a key player in non-alcoholic steatohepatitis. J Hepatol 2017;67:328–338.
[21] Miura K, Yang L, van Rooijen N, Ohnishi H, Seki E. Hepatic recruitment of macrophages promotes nonalcoholic steatohepatitis through CCR2. Am J Physiol Gastrointest Liver Physiol 2012;302:G1310–G1321.
[22] Francque S, Szabo G, Abdelmalek MF, Byrne CD, Cusi K, Dufour JF, et al. Nonalcoholic steatohepatitis: the role of peroxisome proliferator-activated receptors. Nat Rev Gastroenterol Hepatol 2021;18:24–39.
[23] Stienstra R, Saudale F, Duval C, Keshtkar S, Groener JE, van Rooijen N, et al. Kupffer cells promote hepatic steatosis via interleukin-1beta-dependent suppression of peroxisome proliferator-activated receptor alpha activity. Hepatology 2010;51:511–522.
[24] Montagner A, Polizzi A, Fouche E, Ducheix S, Lippi Y, Lasserre F, et al. Liver PPARalpha is crucial for whole-body fatty acid homeostasis and is protective against NAFLD. Gut 2016;65:1202–1214.
[25] Francque SM, Bedossa P, Ratziu V, Anstee QM, Bugianesi E, Sanyal AJ, et al. A randomized, controlled trial of the pan-PPAR agonist lanifibranor in NASH. N Engl J Med 2021;385:1547–1558.
[26] Faletti L, Peintner L, Neumann S, Sandler S, Grabinger T, Mac Nelly S, et al. TNFalpha sensitizes hepatocytes to FasL-induced apoptosis by NFkappaB-mediated Fas upregulation. Cell Death Dis 2018;9:909.
[27] Beier K, Volkl A, Fahimi HD. TNF-alpha downregulates the peroxisome proliferator activated receptor-alpha and the mRNAs encoding peroxisomal proteins in rat liver. FEBS Lett 1997;412:385–387.
[28] Cawthorn WP, Sethi JK. TNF-alpha and adipocyte biology. FEBS Lett 2008;582:117–131.